NACA RM L55A05a

RESEARCH MEMORANDUM

INVESTIGATION AT TRANSONIC SPEEDS OF AERODYNAMIC CHARACTERISTICS OF A SEMICIRCULAR AIR INLET IN THE ROOT OF A 45° SWEPTBACK WING

By Charles D. Trescot, Jr. and Arvid L. Keith, Jr.

Langley Aeronautical Laboratory
Langley Field, Va.

NATIONAL ADVISORY COMMITTEE
FOR AERONAUTICS
WASHINGTON

March 23, 1955
Declassified February 10, 1958

NACA RM L55A05a

NATIONAL ADVISORY COMMITTEE FOR AERONAUTICS

RESEARCH MEMORANDUM

INVESTIGATION AT TRANSONIC SPEEDS OF AERODYNAMIC CHARACTERISTICS OF A SEMICIRCULAR AIR INLET IN THE ROOT OF A 45° SWEPTBACK WING

By Charles D. Trescot, Jr. and Arvid L. Keith, Jr.

SUMMARY

An investigation has been made in the Langley transonic blowdown tunnel at Mach numbers from 0.63 to 1.41 to determine increments in lift, drag, and pitching moment of a sweptback semicircular air inlet installed in the root of a 45° sweptback wing and to study the total-pressure recovery characteristics of the inlet. The test range of angle of attack and mass-flow ratio varied from 0.4° to 8.5° and 0.36 to 0.91, respectively. The maximum engine-face total-pressure ratio at a mass-flow ratio of 0.80 was 0.97 at subsonic speeds. Increases in Mach number to 1.4 reduced the maximum total-pressure ratio to 0.84 through interaction of the inlet-shock and fuselage-nose boundary layer. The transonic drag rise of the inlet configuration was a maximum of 0.004 greater in external-drag coefficient than the basic wing-body configuration at low angles of attack. In general, installation of the inlet had little effect on the pitching-moment or lift characteristics except for Mach numbers between 0.98 and 1.10 where pitch-up occurred at somewhat lower lift coefficients for the inlet configuration than for the basic configuration. The performance index of the semicircular inlet was considerably lower at comparable design conditions than that of a triangular-shaped (NACA Research Memorandum L52H08a) and a semielliptical-shaped (NACA Research Memorandum L53J22a) inlet because of lower pressure recovery and higher drag increments.

INTRODUCTION

A series of investigations at transonic speeds has been undertaken to evaluate the aerodynamic characteristics of various-shaped sweptback inlets installed in the root of a 45° sweptback wing. The investigations of a triangular- and a semielliptical-shaped inlet have been reported in references 1, 2, and 3. Results of these studies show that, in general,

the addition of the inlet to a basic sweptback wing-body combination can be accomplished with little or no cost in external drag. The results show further that the total-pressure ratio at an assumed jet-engine compressor-face station remained high until the inlet shock strength became of sufficient magnitude to cause the fuselage-nose boundary layer to thicken and, subsequently, to separate.

For the present investigation, a sweptback semicircular-shaped inlet installed in the root of a 45° sweptback wing has been investigated at Mach numbers ranging from about 0.63 to 1.41, at angles of attack varying from 0.4° to 8.5°, and at mass-flow ratios from 0.36 to 0.91. The tests were conducted in the Langley transonic blowdown tunnel. Measurements included total-pressure distributions at the inlet and exit, lift, drag, and pitching moment. The results are compared with the basic sweptback wing-body combination and the two previously tested inlets of references 1 and 2.

SYMBOLS

C_{D_b} drag coefficient of basic body of revolution, $\frac{\text{Drag}}{q_o S}$

$C_{D_{wb}}$ drag coefficient of basic wing-body combination

$\Delta C_{D_{ext}}$ difference in drag coefficient obtained between basic and inlet configurations at the same angle of attack and Mach number after effects of internal flow and air exit have been removed from inlet configuration (see appendix of ref. 1)

$C_{L_{wb}}$ lift coefficient of basic wing-body combination, $\frac{\text{Lift}}{q_o S}$

$\Delta C_{L_{ext}}$ difference in lift coefficient obtained between basic and inlet configurations at the same angle of attack and Mach number after effects of internal flow and air exit have been removed from inlet configuration (see appendix of ref. 1)

$C_{m_{wb}}$ pitching-moment coefficient of basic wing-body combination taken about quarter chord of mean aerodynamic chord, $\frac{\text{Pitching moment}}{q_o S \bar{c}}$

ΔC_m difference in pitching-moment coefficient obtained between basic and inlet configurations at the same lift coefficient and Mach number after effects of air exit have been removed from inlet configuration (see ref. 2)

$C_{T_{ideal}}$ engine thrust coefficient based on ideal condition, $\frac{\overline{H}}{H_o} = 1.0$

$\frac{\overline{H}}{H_o}$ integrated total-pressure recovery weighted with respect to

mass flow, $\frac{\int_A \frac{\rho V}{\rho_o V_o} \frac{H}{H_o} dA}{\int_A \frac{\rho V}{\rho_o V_o} dA}$

$\frac{H - p_o}{H_o - p_o}$ impact-pressure ratio

$\frac{m_i}{m_o}$ mass-flow ratio, defined as ratio of total internal mass flow to mass flow through a free-stream tube equal in area to minimum projected area of both inlet openings

A area

A_i projected frontal area of both inlet openings normal to flow direction, defined by minimum inner-lip radius and fuselage wall

$\bar{c}$ mean aerodynamic chord of basic wing, 4.462 in.

F frontal area of fuselage, 7.07 sq in.

H total pressure

M Mach number

m rate of internal mass flow

p static pressure

q dynamic pressure, $\frac{1}{2}\rho V^2$

R Reynolds number based on $\bar{c}$

S	basic wing area, 80.7 sq in.
$\frac{V}{V_i}$	ratio of local velocity parallel to surface and within boundary layer to local velocity parallel to surface at outer edges of boundary layer at inlet measuring station
V	velocity
X	distance parallel to fuselage center line
Y	distance perpendicular to a plane through wing chord
α	angle of attack
ρ	mass density

Subscripts:

c	compressor-face station
i	inlet
o	free stream
x	jet-exit station

MODEL CONFIGURATIONS

Basic model.- A photograph of the basic model is shown as figure 1(a). The model consisted of a wing with a 45° quarter-chord sweep mounted at zero incidence in the midwing position on a fuselage of fineness ratio 6.7. The wing was composed of NACA 65A008 airfoil sections in the streamwise direction, had an aspect ratio of 4.032, and had no twist and no dihedral. The basic fuselage was formed by rotating an NACA 65_2A015 airfoil section about its chord line and is identical to that of references 1 to 3.

Inlet model.- The semicircular wing-root inlet model (figs. 1(b) to 1(d)) was obtained by installing a seminacelle with closed afterbody in the wing root of the basic sweptback wing-body combination. The inlet section or nacelle forebody was essentially a seminose inlet which was skewed in two planes and produced both a sweptback inlet (sweep angle of 46.7°, same as basic-wing leading edge) and a staggered inlet (stagger angle of 20°). Elliptical ordinates were used to fair the external lip shapes back to the nacelle maximum thickness. The distance from the

inlet-lip leading edge to the position of maximum thickness was maintained constant. In combination with the inlet sweep and stagger, this constant distance resulted in an approximately triangular-shaped flat spot on both upper and lower external surfaces between the end of the elliptical ordinates and the beginning (maximum-thickness station) of the afterbody. The afterbody was composed of the rear section of an NACA 663-018 airfoil section rotated about its chord line.

Elliptical ordinates were also used to fair the inner lip surfaces back to the minimum inlet area. Dimensions of the inlet are shown in table I.

The inboard wall of the inlet (spanwise station 1.200) required that alterations to the basic fuselage nose shape be incorporated to avoid sharp discontinuities in contour. A flat section immediately ahead of the inlet plane was incorporated and was faired to the original nose shape at fuselage station 2.500. (See fig. 2.)

The projected frontal area of the inlets relative to the fuselage $\left(\frac{A_i}{F} = 0.167\right)$ was the same as that for the triangular and semielliptical inlets tested in references 1 and 2, respectively. Inasmuch as the inlets are assumed to meet the airflow requirements of a single engine, the two semicircular ducts were designed to merge at an assumed engine compressor face. Neither the internal ducting nor the area ratio at this station, $\frac{A_c}{A_i} = 1.042$, simulated that required for an actual turbojet engine installation because of model space limitation. The duct behind the assumed compressor face was circular and led to an exit in the tail of the fuselage. As shown in figure 2, three exit areas $\left(A_x/A_c = 1.00, 0.75, \text{ and } 0.50\right)$ were used to vary the internal flow rate.

APPARATUS AND METHODS

Pressure and force measurements.- The inlet model was instrumented with rakes of total- and static-pressure tubes in the right inlet and at the exit measuring station (fig. 3) and a three-component (lift, drag, and pitch) internal strain-gage balance; a dummy rake was installed in the left inlet to avoid asymmetrical flow due to rake blockage. The pressures and forces were measured and recorded photographically in the same manner as in reference 1 by using rapid-response equipment. The force data were corrected for the effects of internal flow and the effects of the jet exit in accordance with the methods presented in references 1 and 2.

Unlike the previous wing-root-inlet investigations, pressure instrumentation was not installed at the assumed engine-compressor-face station. Elimination of the rake was considered desirable because higher internal flow rates could be attained and the number of tests could be reduced; this arrangement permitted determination of the average total-pressure ratio and the model forces simultaneously where separate tests were required previously. The inlet pressure-tube rakes were removed when the total-pressure recovery and force tests were made. In order to permit direct comparison of the average total-pressure ratios of the present inlet configuration with those of references 1 and 2, a correlation of the compressor-face and exit total pressures was made with published and unpublished data of references 2 and 3. It was determined that the total pressure loss between the two stations was less than 2 percent of the free-stream total pressure through the range of test variables. Therefore, average total-pressure ratios equivalent to those at the compressor-face station were obtained for the present inlet simply by adding the loss factor between stations to the average total-pressure ratios obtained at the exit.

Tests.- The tests were conducted in the Langley transonic blowdown tunnel at stagnation pressures ranging from 43 to 60 pounds per square inch absolute. The range of test variables and the estimated maximum errors in the measured coefficients based on scatter and repeatability of data are given in the following tables:

Variable	Range	Maximum estimated error
M_o	0.63 to 1.41	± 0.01
R	5.5×10^6 to 7.4×10^6	(± 2 percent due to variation in stagnation temperature)
α	0.4° to 8.5°	$\pm 0.1^\circ$
$\frac{m_i}{m_o}$	0.36 to 0.91	± 0.02

Measured coefficient	Maximum estimated error
ΔC_L	± 0.01
ΔC_D	± 0.001
ΔC_m	± 0.003
$\frac{H - p_o}{H_o - p_o}$	± 0.005
$\frac{\overline{H}}{H_o}$	± 0.01[a]

[a]At inlet mass flows $\frac{m_i}{m_o} \geqq 0.8$, maximum error is estimated to be ± 0.005.

The large ratio of model to tunnel size precluded obtaining force data which were exactly equivalent to free-air data at any speed. Furthermore, at all supersonic speeds the model forces were subject to the effects of tunnel-wall reflections of model compressions and expansions. These effects caused changes in drag coefficient with Mach number which were sometimes large and rather abrupt. As pointed out in reference 3, most of the effect of the wall-reflected disturbances on drag occurred on the body alone so that subtraction of body-alone drag data from that of the wing-body combinations resulted in variations of the drag characteristics with Mach number more nearly representative of the variations expected in free air. In any event although the absolute force coefficients may not be correct, comparisons between the various configurations are believed correct to the quoted accuracy except for the range of Mach number between 1.08 and 1.22 where the reflections crossed the inboard wing panels. (See ref. 3.)

RESULTS AND DISCUSSION

Internal Pressures

Flow at inlet.- The shape of the fuselage nose just ahead of the inlet was slightly different from that tested in references 1 and 2 because of the large flat section required by the present semicircular inlet. (See section entitled "Inlet Model.") Pressure distributions

over the nose, however, showed that the Mach number just ahead of the inlet compression shock was approximately free stream as was the case for the other configurations.

Contours of impact-pressure ratio at the inlet are presented in figure 4 for the test range of Mach number at mass-flow ratios of about 0.70 and 0.55 and angles of attack of 0.4° and 4.6°. At subsonic speeds and $\alpha = 0.4^\circ$, the impact pressures were nearly stream value over the major part of the inlet at the highest mass-flow ratio. The lower pressure ratios in the inboard section show the boundary-layer growth over the fuselage nose.

With increases in Mach number above 1.0, a shock was formed ahead of the inlet and its interaction with the boundary layer caused substantial increases in the boundary-layer thickness. Further increases in Mach number and consequently shock strength resulted in boundary-layer separation. At a Mach number of 1.4, most of the inlet was involved with the boundary layer, and reversed or unsteady flow was present within the boundary layer through the entire test range of mass-flow ratio, (figs. 4 and 5); the maximum test value of m_i/m_o at this Mach number was 0.71 with the inlet pressure-tube rakes installed. Reductions in m_i/m_o caused the boundary layer to be affected adversely at all Mach numbers because of an increase in the positive pressure gradient ahead of the inlet. As will be discussed in the following section, twin-duct instability occurred at reduced mass-flow ratios. In fact, for the lowest test mass-flow ratio of about 0.35, twin-duct instability practically eliminated the flow through one of the inlets at the higher Mach numbers so that an individual inlet mass-flow ratio of about 0.70 was obtained through one of the inlet sides. The inlet pressure contours for this case, although not presented, were very nearly similar to those obtained at the maximum flow rate. The main effect of increasing the angle of attack was to reduce the inboard pressures somewhat and to shift this region of low pressure to the lower part of the inlet.

Figure 4 indicates also that the impact-pressure ratios, even at the highest Mach numbers, were nearly stream value in regions of the inlet which were free of boundary layer. The inlet shock would necessarily be inclined because of the inlet sweep, and high pressure ratios would be expected behind this type of compression. For the present low-aspect-ratio inlet, however, it is not clear whether the high pressure ratios in the outboard parts of the inlet were due only to the inlet sweep effect or were also partially due to the lambda-type shock accompanying boundary-layer separation. At any rate, a maximum individual impact-pressure ratio of 0.99 was measured in the outboard end of the inlet compared with an impact-pressure ratio of 0.94 behind a normal shock at $M_o = 1.40$. Inasmuch as the greater part of the total-pressure losses for the present inlet were due to shock-boundary-layer effects, increases in average total-pressure recovery can obviously be attained by means of some

type of boundary-layer control. If the measured high recoveries at the outboard inlet stations were due primarily to the inlet sweep, boundary-layer control would probably result in average recoveries greater than the normal-shock values. Inclusion of a more efficient external compression would, of course, increase the attainable pressure recovery.

Flow at compressor-face station.- Average total-pressure ratios at the assumed compressor-face station are presented in figure 6 as a function of Mach number and mass-flow ratio at several angles of attack. This pressure ratio includes the cumulative result of losses due to the fuselage-nose boundary layer, the compression ahead of the inlet, and the internal-duct losses. For a mass-flow ratio of 0.8 and an angle of attack of 0.4°, the total pressures were a maximum ($0.97H_0$) at the lowest test speed (fig. 6(a)). With increases in free-stream Mach number above 1.10, the losses due to shock-boundary-layer interactions began to be severe. At a free-stream Mach number of 1.40, the average total pressure was only $0.84H_0$, a value about $0.12H_0$ below the recovery across a normal shock.

Reduction in mass-flow ratio at subsonic speeds caused only small changes in the total pressures (fig. 6(b)). With increases in Mach number, however, the effects of a decrease in mass-flow ratio became more severe. At the highest test Mach number, the total-pressure ratio was decreased from 0.84 to 0.78 with reductions in mass-flow ratio from 0.80 to 0.60. Further reductions in mass flow resulted in unstable flow in the two inlets of the type discussed in reference 4 (the dashed part of the curves). Calculations of the mass-flow ratio from the rakes at both the inlet and exit stations indicated that nearly all the internal flow was being taken in through one inlet at the lowest system mass-flow ratio ($m_i/m_0 \approx 0.35$). The initiation of twin-duct instability is believed to occur for the present inlet at a flow rate somewhat higher than that for the previous inlets of references 1 and 2 ($m_i/m_0 \approx 0.50$) as indicated by exit-pressure fluctuations that were noted at mass-flow ratios up to about 0.64.

Increases in angle of attack from 0.4° to 8.5° caused negligible changes in the average total-pressure ratio at subsonic and sonic speeds. At supersonic speeds, the changes were still small (on the order of about $0.02H_0$ at $M_0 = 1.40$). The angle-of-attack effects were also nearly constant with mass-flow-ratio variations.

Lift and pitching moment.- Installation of the semicircular inlet caused no consistent significant changes in the lift characteristics of the basic wing-body combination (fig. 7). Comparison of the pitching-moment characteristics, however, (fig. 8) shows that the inlet installation effected a general slight decrease in the longitudinal stability throughout the tested Mach number range. A similar forward shift in

center of pressure did not occur with installation of the semielliptical inlet of reference 2 because of the positive loading over the large trailing-edge fillet incorporated as part of the inlet design. For the range of Mach number between 0.98 and 1.10, pitch-up occurred for the semicircular inlet configuration at somewhat lower lift coefficients than for the basic configuration. Effects of mass-flow-ratio variations on pitching moment were generally almost within the experimental accuracy at lift coefficients below that required for pitch-up.

External drag.- As pointed out earlier, the drag coefficients of the basic body alone have been subtracted from those of both the inlet and basic configurations to obtain variations with Mach number more nearly representative of drag-coefficient variations in free air. The external-drag coefficients of the inlet configuration at the design mass-flow ratio and of the basic wing-body configuration were about the same at subsonic speeds (fig. 9), and the initiation of the drag rise occurred at about the same Mach number at low angles of attack. At the peak of the drag rise for the lower two angles (M_0 between 1.02 and 1.05), however, the inlet-configuration drag coefficients were somewhat greater with the maximum increase being about $\Delta C_D = 0.004$. For higher speeds, the increase in drag coefficient due to the inlet was less than this value. As pointed out in reference 3, some of the increment in the transonic drag rise due to the inlet installation at low and moderate lifting conditions can probably be eliminated by indenting the fuselage an amount equal to the total cross-sectional area added by the inlet less the area of the entering free-stream tube.

Increases in angle of attack above 4.6° resulted in substantially higher drag increments due to installation of the inlet. The maximum measured increment occurred at $\alpha = 6.6°$ and was 0.013 at $M_0 \approx 1.05$. The level of the measured coefficients for the 8.5° angle-of-attack case was so great that it indicated large additional tunnel blocking especially near sonic speeds. The increments here (shown dotted in figs. 9(a) and (b)) are probably not correct.

The effect of inlet mass-flow ratio on the drag increment due to the inlet installation indicates that the lowest drag will occur at the highest flow rate (fig. 9(b)). Inasmuch as the total-pressure-recovery curves also indicate a trend toward higher recovery with increasing inlet mass-flow ratio, an inlet of this type should be designed for as high a flow rate as possible (avoiding inlet choke) for most efficient operation at supersonic speeds.

Inlet Performance

In order to appraise the performance of an air inlet installation, a parameter was chosen that accounts for both the inlet total-pressure

recovery and drag. The parameter used in this paper, defined as the performance index, is the ratio of net propulsive thrust produced by an engine in conjunction with the inlet considered to the thrust of the same engine with an ideal inlet where the ideal inlet would produce 100-percent pressure recovery and zero drag increment. The performance index for the present inlet was obtained by converting the losses in total-pressure recovery to losses in thrust by using a curve similar to that presented in reference 5. The pressure-recovery thrust losses were then summed with the drag increments due to inlet installation. The increments in drag due to inlet installation $\Delta C_{D_{ext}}$ and the losses in total-pressure ratio $\frac{\Delta\bar{H}}{H_o}$ used to obtain the performance index for the present inlet are presented in figure 10. For comparative purposes, similar values are presentented in figure 10 for the inlets of references 1 and 2. The schedule of the inlet mass-flow ratio of a 10,000-pound static-thrust turbojet engine - which was matched with the inlet at a Mach number of 1.40, inlet mass-flow ratio of 0.8, and altitude of 35,000 feet - is also shown in figure 10 for the 35,000-foot altitude condition.

The performance index of the semicircular inlet is presented in figure 11 as a function of Mach number at angles of attack of 0.4° and 4.6°. The ideal thrust schedule of the turbojet engine (in coefficient form based on basic wing area) that was used in the calculations through the Mach number range considered is also presented in figure 11; afterburning was assumed at Mach numbers of 0.90 and above. The results indicate that rather good performance can be obtained at the lowest angle of attack up to a Mach number of about 1.15. With further increases in Mach number, the performance index drops off rapidly for the semicircular inlet, largely because of the increasing losses in total-pressure recovery (fig. 10). Increasing the angle of attack to 4.6° reduced the general level of performance due both to higher losses in pressure recovery and to a larger drag increment (fig. 10). It should be noted here that the accuracy of the drag data is ±0.001 and that the abrupt changes in the performance curves (fig. 11) follow closely the changes in the drag increment curves of figure 10. As discussed previously, the drag data in the Mach number range between about 1.08 and 1.22 are affected by disturbances reflected in the wing-root region of the models and the data are not strictly comparable.

For comparative purposes, the performance curves of the triangular inlet (ref. 1) and the semielliptical inlet (ref. 2) are also presented in figure 11. The performance of the semicircular inlet is inferior to the performance of both the semielliptical and triangular inlets at all supersonic Mach numbers primarily because of lower internal pressure recoveries. Greater external drag increments are also a contributing factor. Inasmuch as the internal total-pressure losses for all these inlets are due mainly to the fuselage boundary layer, the semicircular

inlet, which had the lowest aspect ratio and thereby the greatest percentage of inlet area influenced by the boundary layer, should have the lowest performance. It should perhaps be mentioned again that incorporation of an efficient external compression or boundary-layer control would probably result in substantial improvements in performance. For example, in reference 2, removal of only 3 percent of the inlet flow through a crude boundary-layer-bleed system increased the average total-pressure recovery at a Mach number of about 1.35 by about $0.03H_0$ which corresponds to an increase in the performance index of about 0.94 compared with 0.90 for the inlet in the original condition.

SUMMARY OF RESULTS

An investigation has been made in the Langley transonic blowdown tunnel at Mach numbers between 0.63 and 1.41 to determine the internal and external aerodynamic characteristics of a sweptback semicircular air inlet installed in the root of a 45° sweptback wing. The results are summarized as follows:

1. The maximum engine-face total-pressure ratio at a mass-flow ratio of 0.80 was 0.97 at subsonic speeds. Increases in Mach number to 1.4 reduced the total-pressure ratio to 0.84 through interaction of the inlet shock and fuselage-nose boundary layer.

2. The transonic drag rise of the inlet configuration was a maximum of 0.004 greater in external-drag coefficient than the basic wing-body configuration at low angles of attack.

3. In general, installation of the inlet had little effect on the pitching-moment or lift characteristics except for Mach numbers between 0.98 and 1.10 where pitch-up occurred at somewhat lower lift coefficients for the inlet configuration than for the basic configuration.

4. The performance index of the semicircular inlet was considerably lower at comparable design conditions than that of a triangular-shaped (NACA Research Memorandum L52H08a) and a semielliptical-shaped (NACA Research Memorandum L53J22a) inlet because of lower pressure recovery and higher drag increments.

Langley Aeronautical Laboratory,
National Advisory Committee for Aeronautics,
Langley Field, Va., December 29, 1954.

REFERENCES

1. Howell, Robert R., and Keith, Arvid L., Jr.: An Investigation at Transonic Speeds of the Aerodynamic Characteristics of an Air Inlet Installed in the Root of a 45° Sweptback Wing. NACA RM L52H08a, 1952.

2. Howell, Robert R., and Trescot, Charles D., Jr.: Investigation at Transonic Speeds of Aerodynamic Characteristics of a Semielliptical Air Inlet in the Root of a 45° Sweptback Wing. NACA RM L53J22a, 1953.

3. Keith, Arvid L., Jr.: Transonic Wind-Tunnel Investigation of the Effects of Body Indentation on the Aerodynamic Characteristics of a Semielliptical Sweptback Wing-Root Inlet Configuration. NACA RM L54A29, 1954.

4. Martin, Norman J., and Holzhauser, Curt A.: Analysis of Factors Influencing the Stability Characteristics of Symmetrical Twin-Intake Air-Induction Systems. NACA TN 2049, 1950.

5. Schueller, Carl F., and Esenwein, Fred T.: Analytical and Experimental Investigation of Inlet-Engine Matching for Turbojet-Powered Aircraft at Mach Numbers Up to 2.0. NACA RM E51K20, 1952.

TABLE I- DESIGN DIMENSIONS OF WING-ROOT INLET CONFIGURATION

(All dimensions in inches)

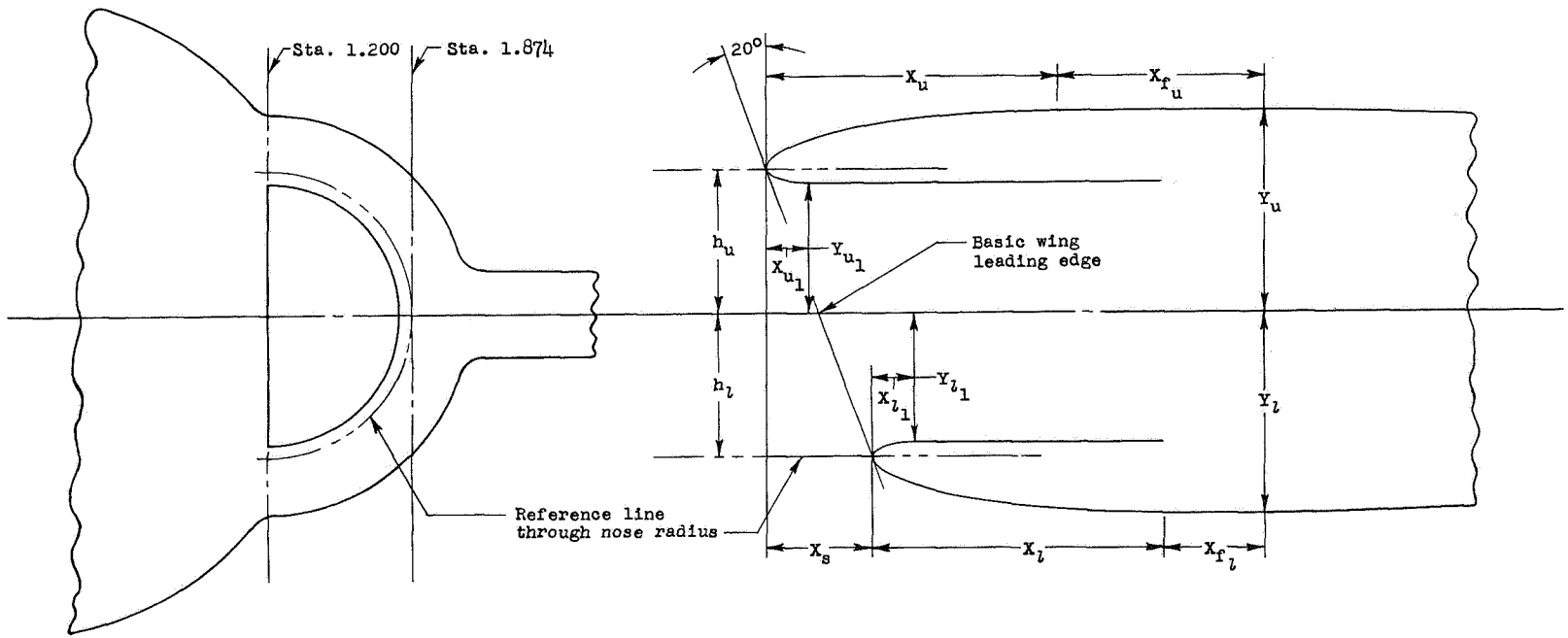

Wing station	External surfaces (a)									Internal surfaces (a)			
	h_u	X_u	Y_u	X_{f_u} (b)	X_s	h_l	X_l	Y_l	X_{f_l} (b)	X_{u_1}	Y_{u_1}	X_{l_1}	Y_{l_1}
1.200	0.674	1.362	0.937	0.960	0.490	0.674	1.362	0.937	0.470	0.169	0.612	0.169	0.612
1.325	.662	1.362	.929	.824	.482	.662	1.362	.929	.342	.188	.598	.188	.598
1.450	.625	1.362	.903	.678	.456	.625	1.362	.903	.222	.188	.558	.188	.558
1.575	.560	1.362	.859	.521	.408	.560	1.362	.859	.113	.188	.483	.188	.483
1.700	.450	1.362	.793	.349	.330	.450	1.362	.793	.019	.188	.352	.188	.352

(a) External and internal nose shapes determined from elliptical ordinates.
(b) Constant ordinate height.

L-78978

(a) Basic model, plan view.

Figure 1.- Photographs of basic and inlet models.

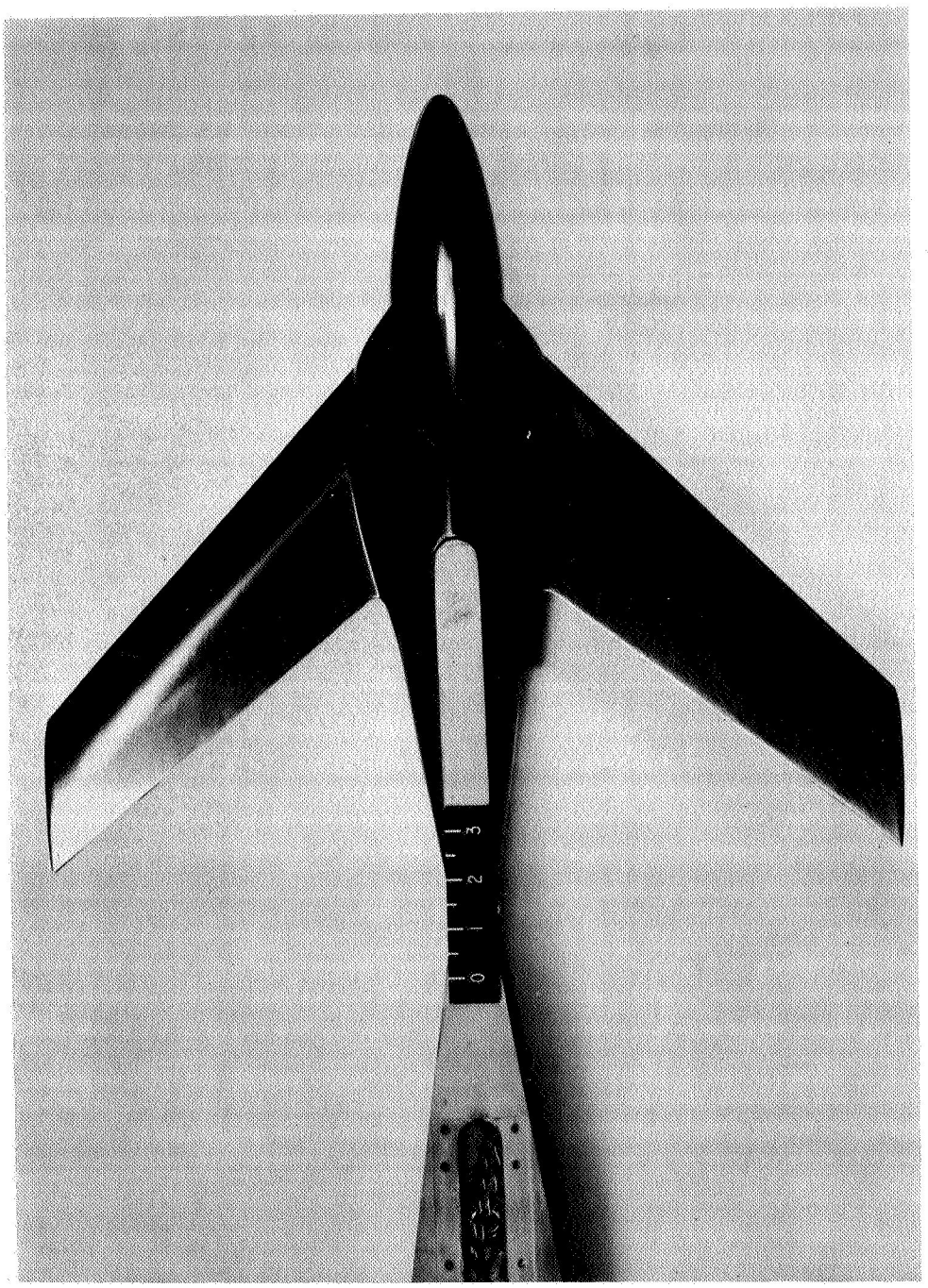

L-81495

(b) Inlet model, plan view.

Figure 1.- Continued.

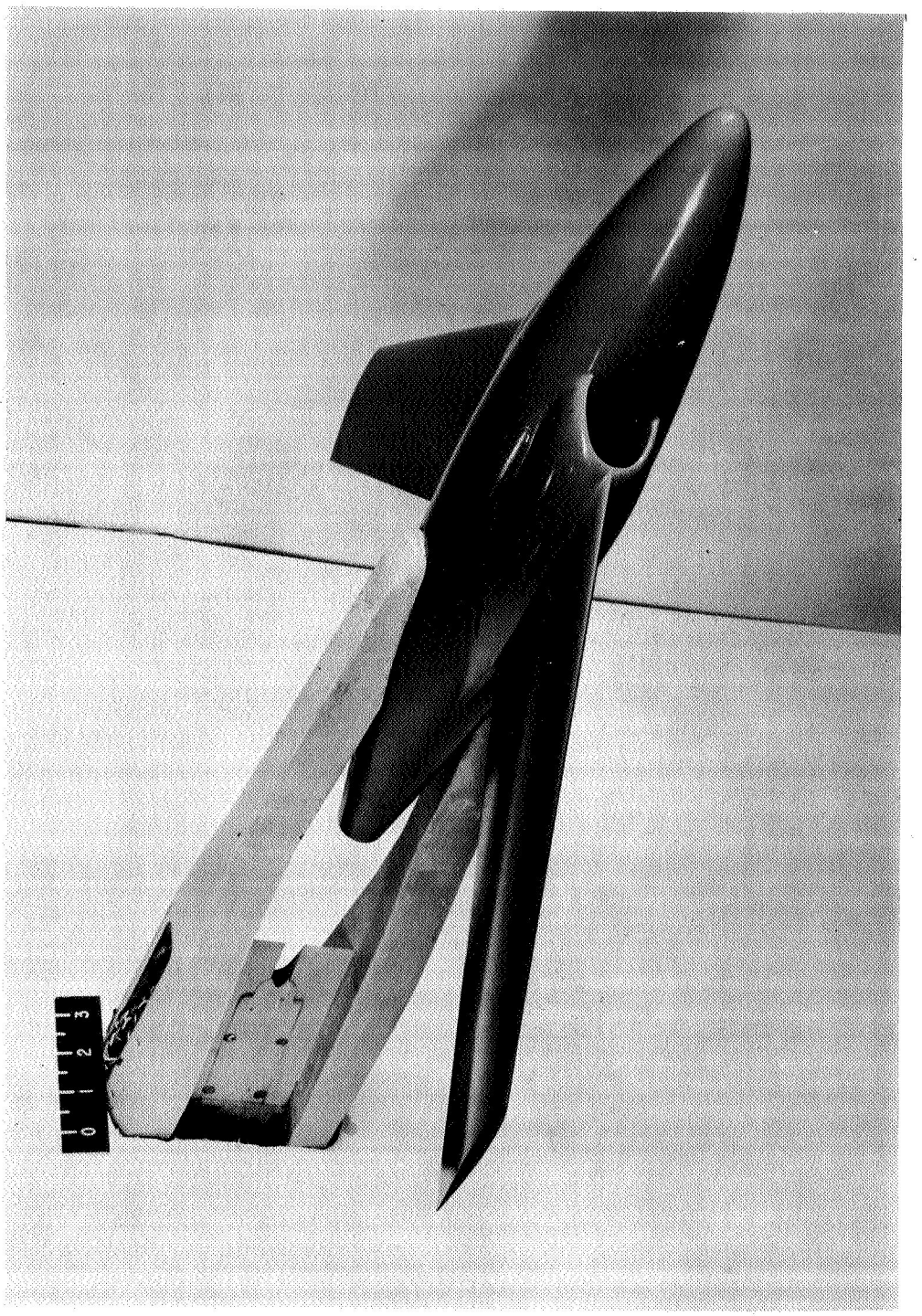

L-81497

(c) Inlet model, 3/4-front view from above.

Figure 1.- Continued.

(d) Inlet model, front view from above. L-81498

Figure 1.- Concluded.

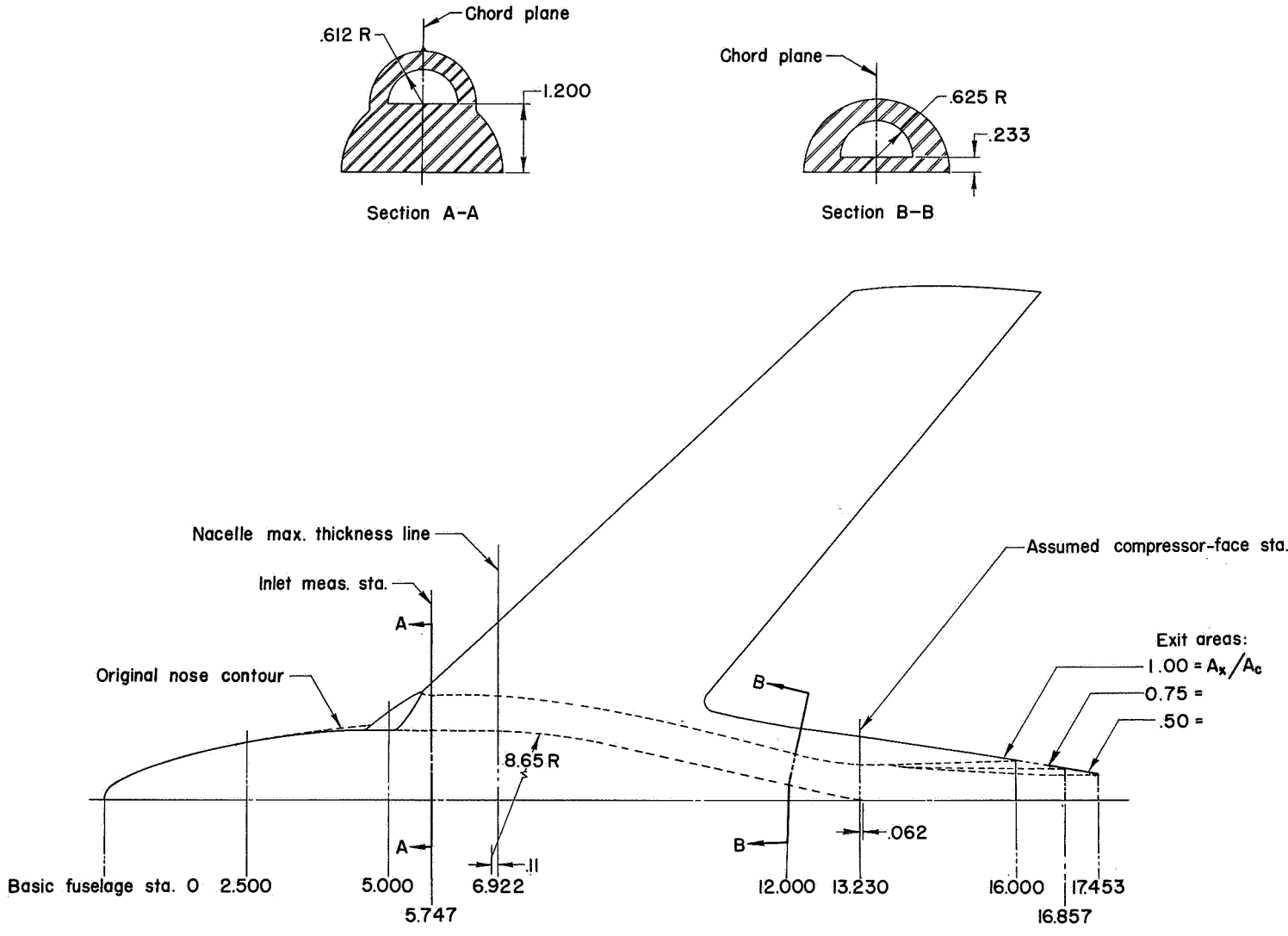

Figure 2.- Plan view of inlet model showing details of internal ducting and exit configuration. All dimensions in inches.

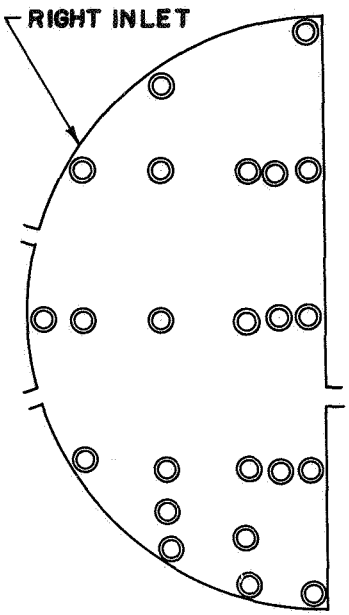

TUBE DISTRIBUTION AT THE INLET MEASURING STATION

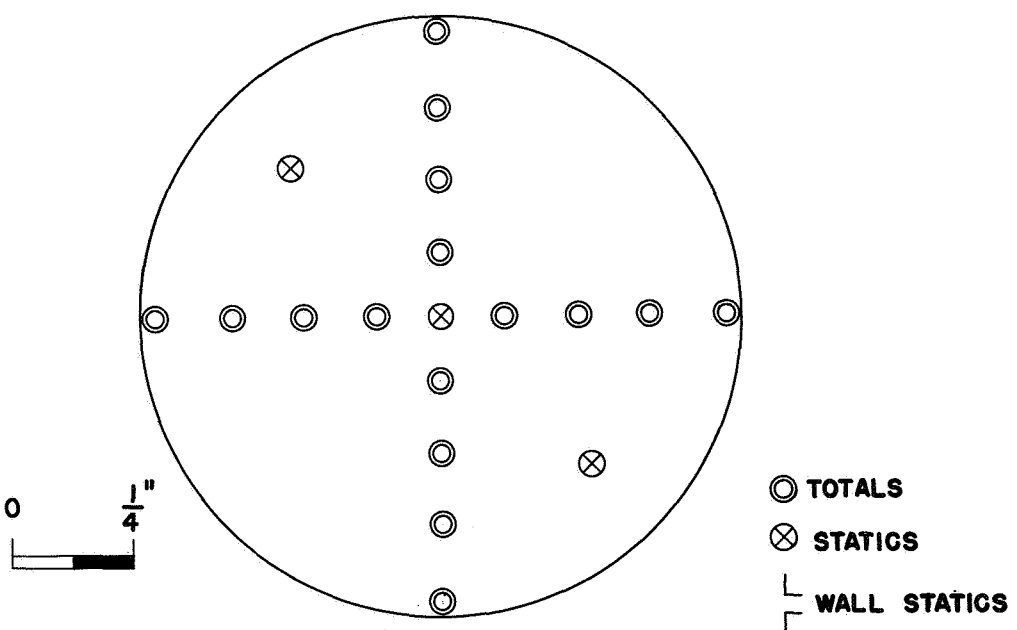

TUBE DISTRIBUTION AT THE EXIT MEASURING STATION

Figure 3.- Total- and static-pressure tube distributions at inlet and exit measuring stations.

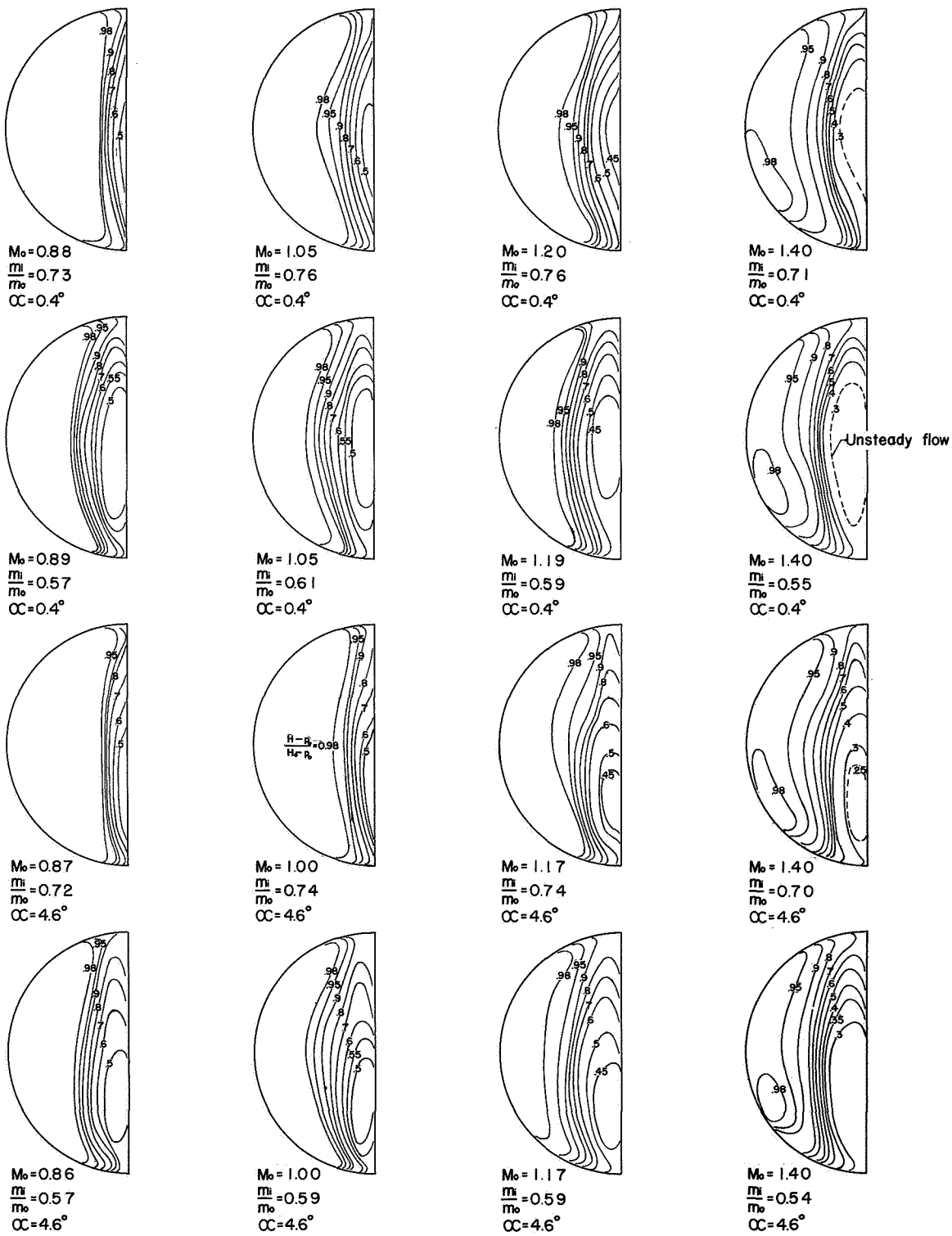

Figure 4.- Contours of impact-pressure ratio at inlet measuring station.

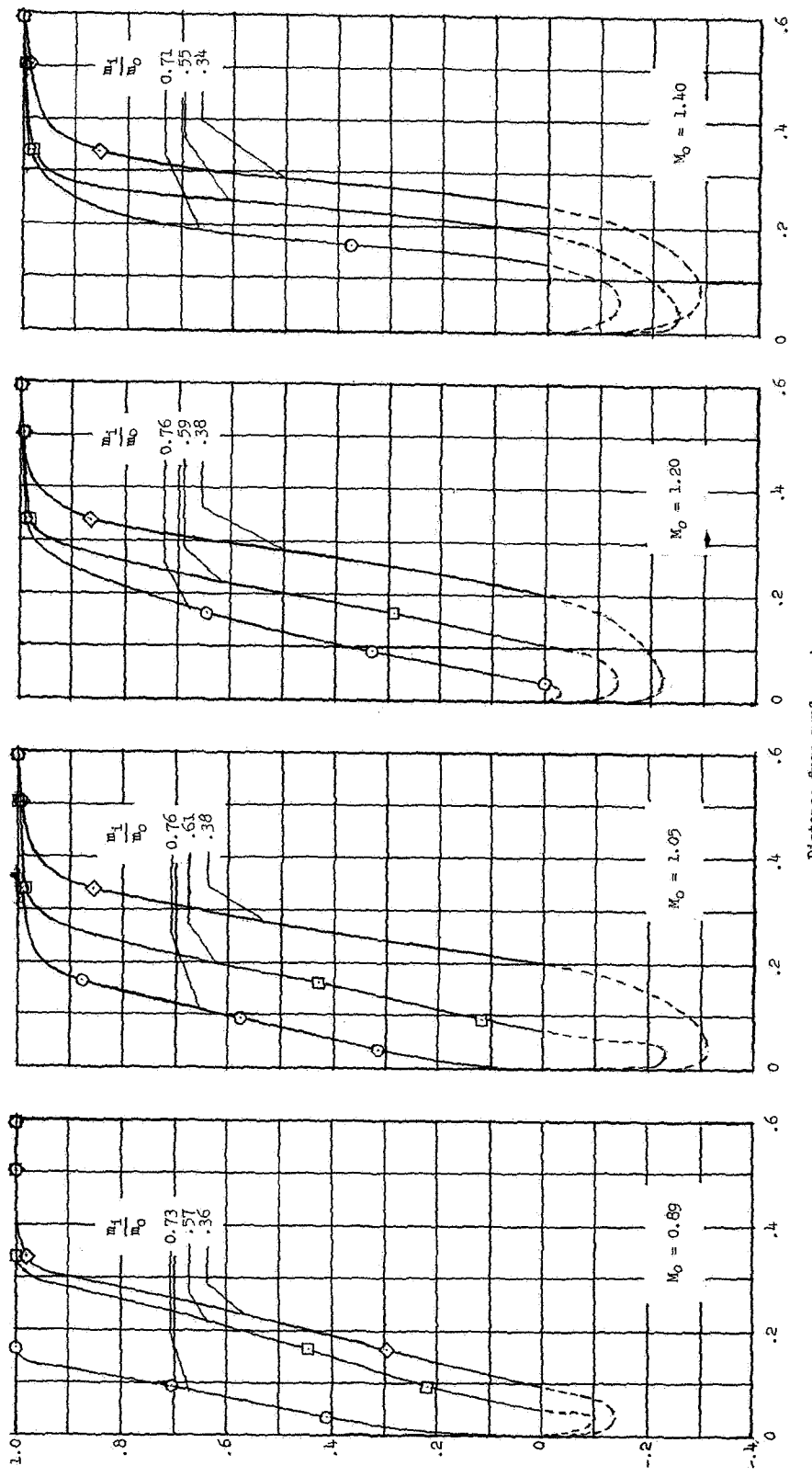

Figure 5.- Velocity profiles in fuselage boundary layer at inlet measuring station.

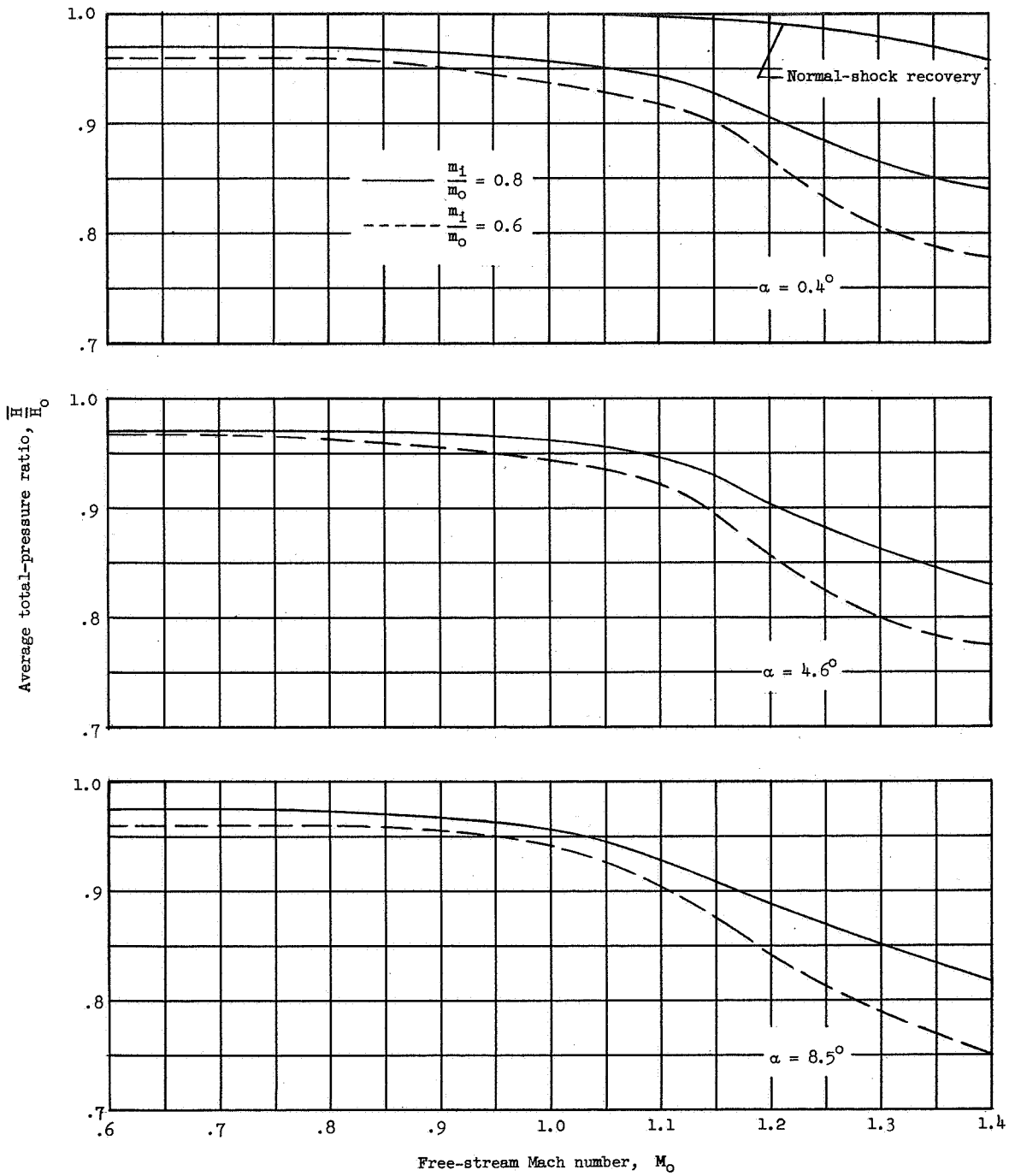

(a) Effect of Mach number and angle of attack.

Figure 6.- Effect of Mach number, angle-of-attack, and mass-flow-ratio variations on weighted total-pressure recovery at the assumed engine compressor face.

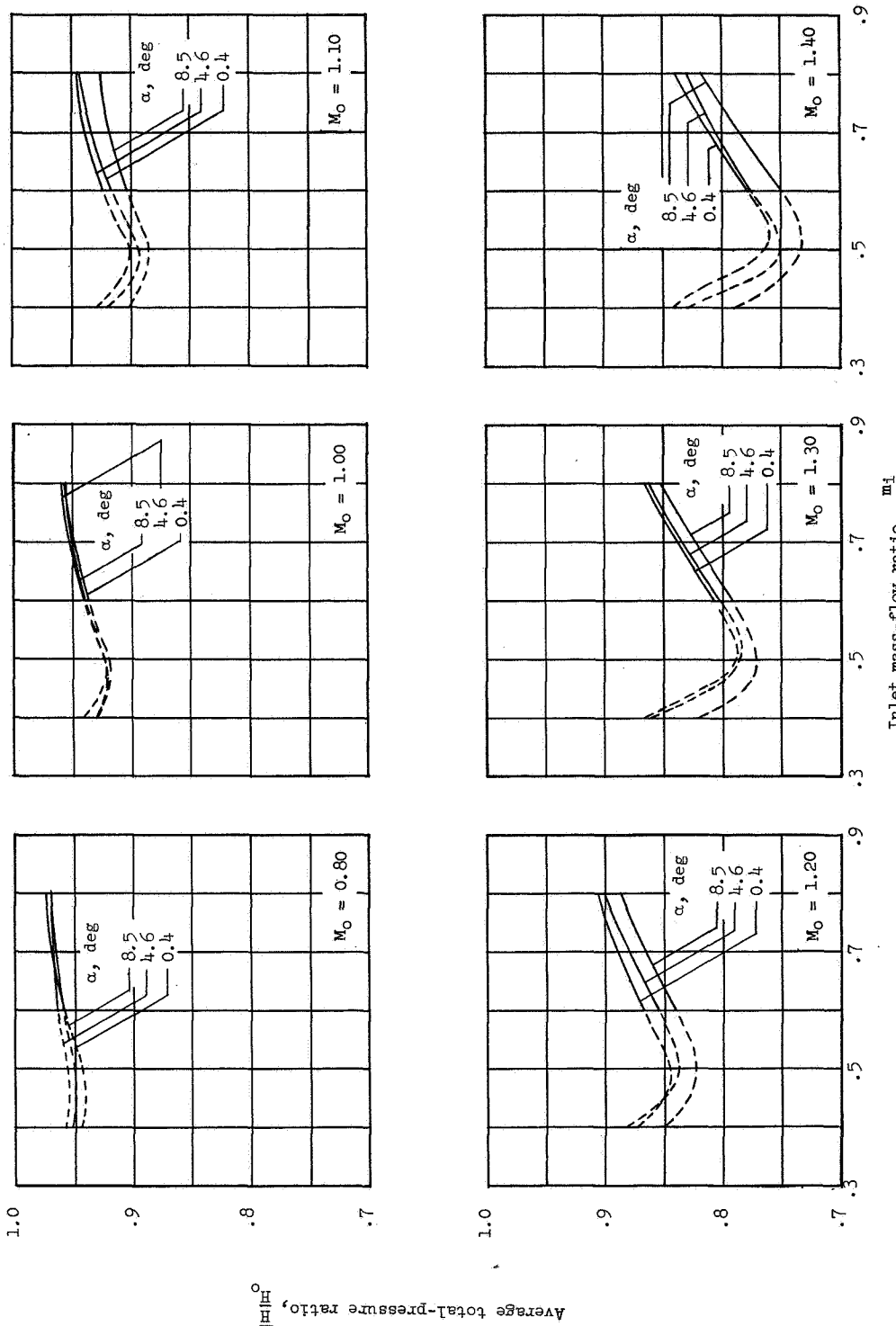

(b) Effect of mass-flow ratio.

Figure 6.- Concluded.

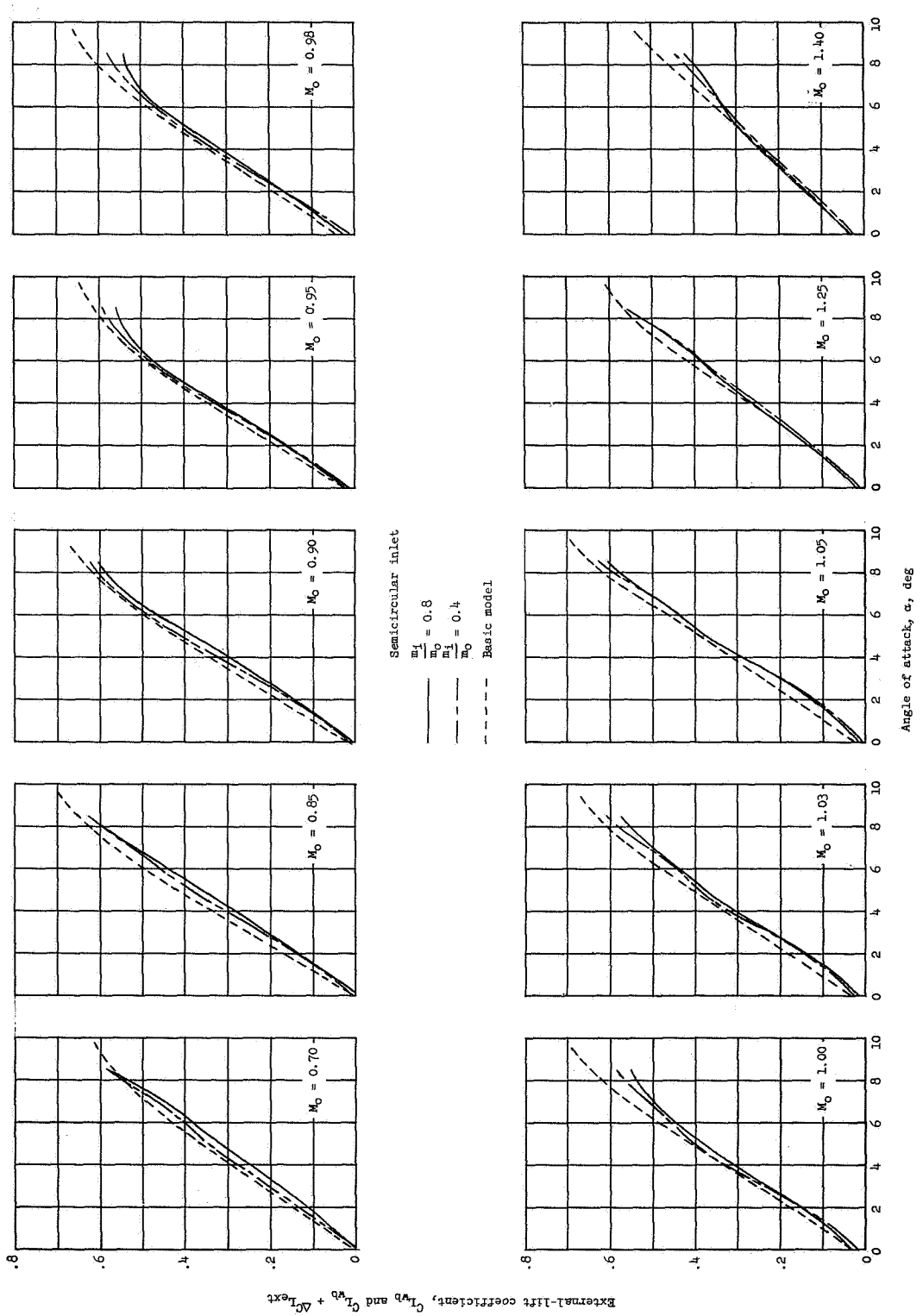

Figure 7.- Effect of angle of attack and inlet mass-flow ratio on lift coefficients for Mach numbers covering test range.

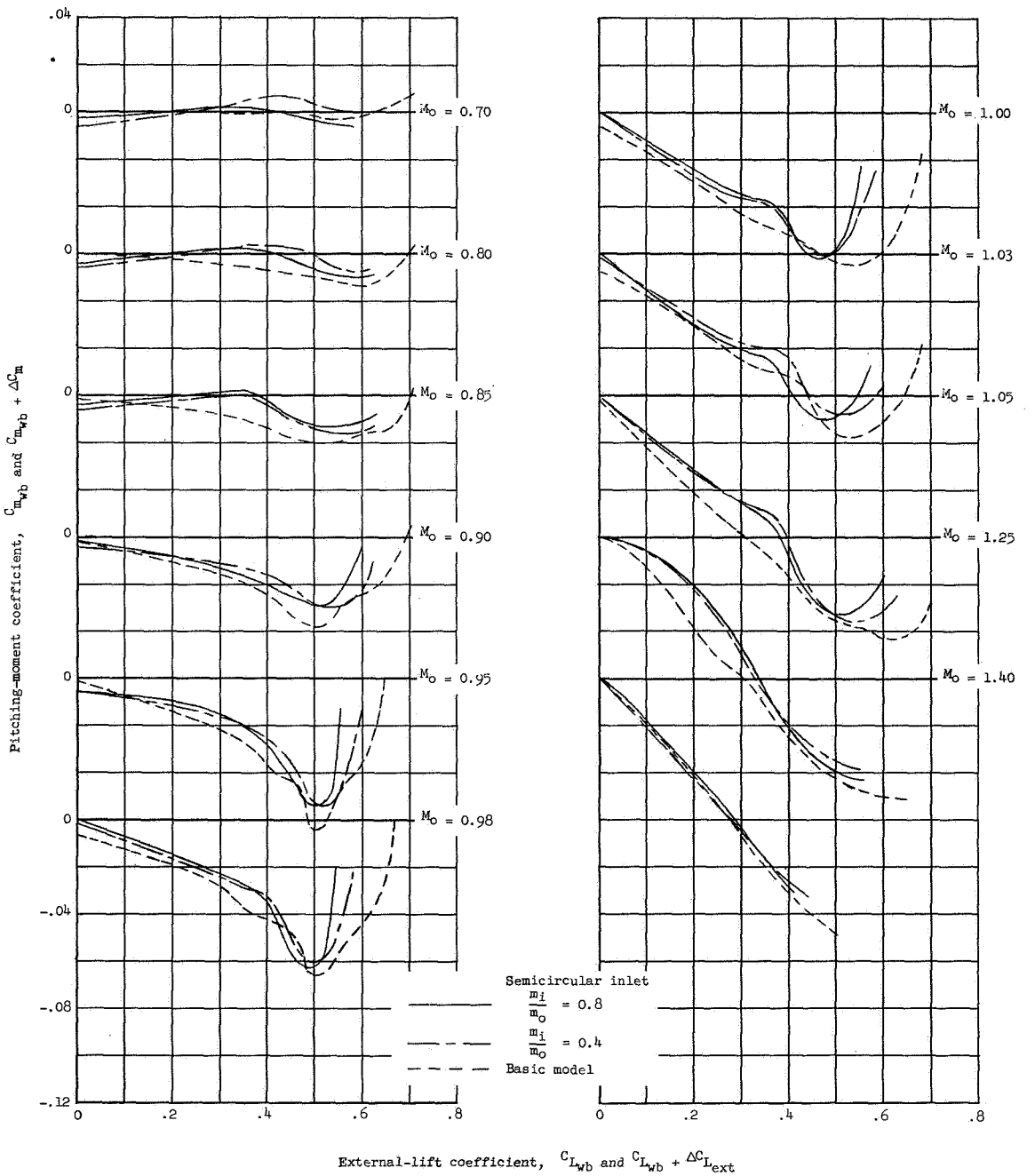

Figure 8.- Comparisons of pitching-moment variation with lift coefficient for basic and inlet configurations for Mach numbers covering test range.

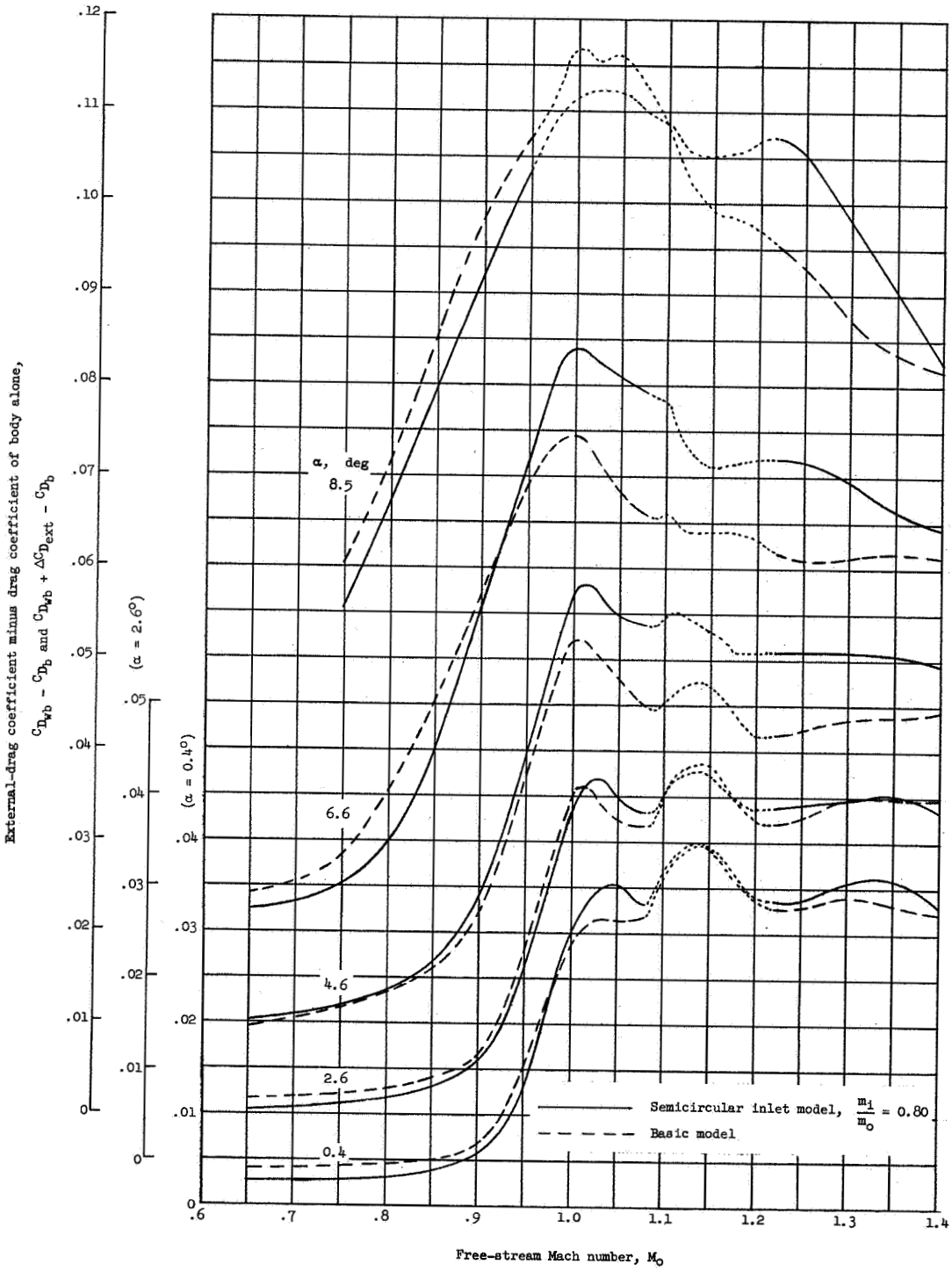

(a) Effect of Mach number.

Figure 9.- Effect of Mach number, angle-of-attack, and inlet mass-flow-ratio variations on external-drag coefficients.

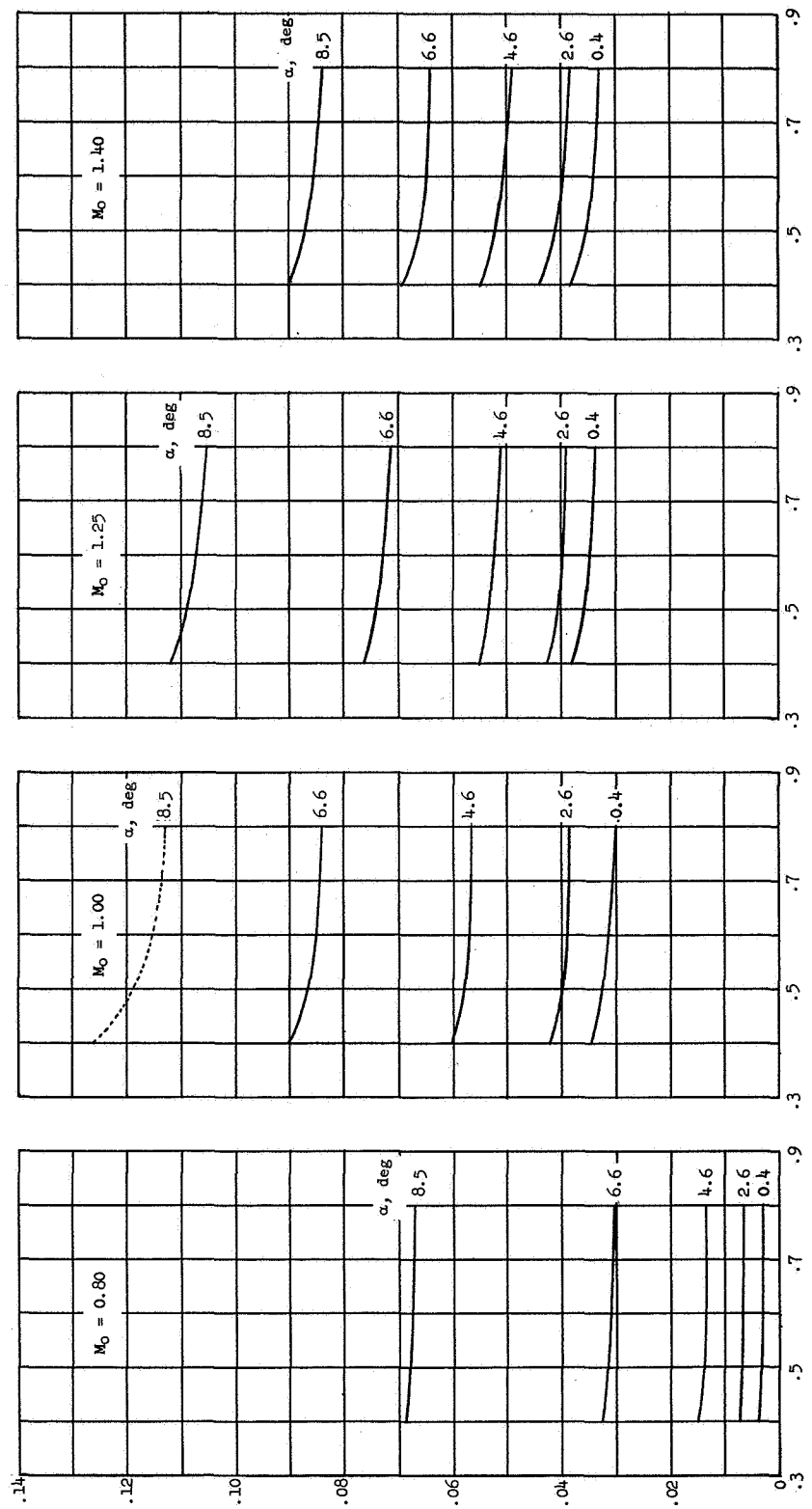

(b) Effect of mass-flow ratio.

Figure 9.- Concluded.

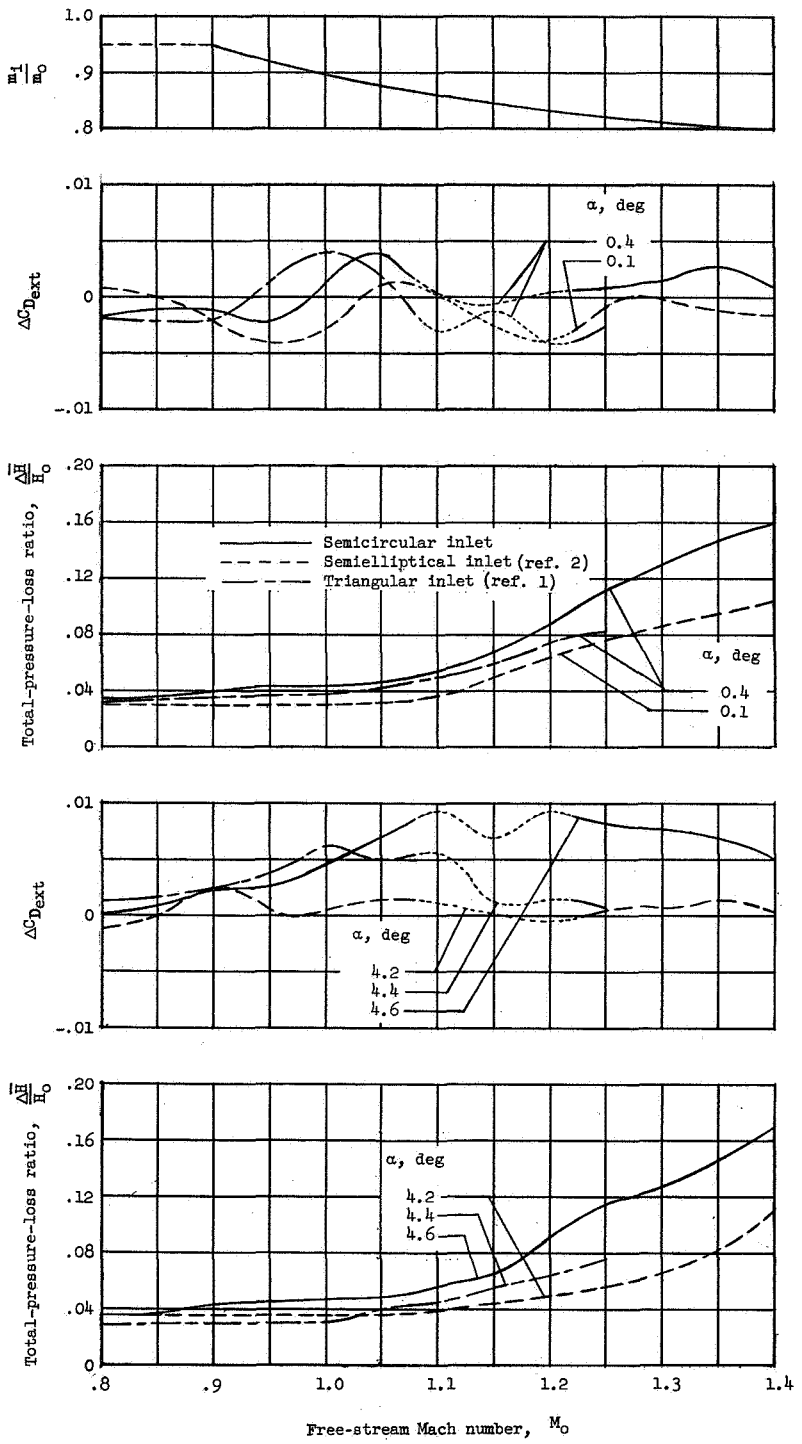

Figure 10.- Comparison of external drag increments and total-pressure-loss ratios with Mach number for semicircular inlet and inlets of references 1 and 2 at mass-flow ratio required by assumed turbojet engine.

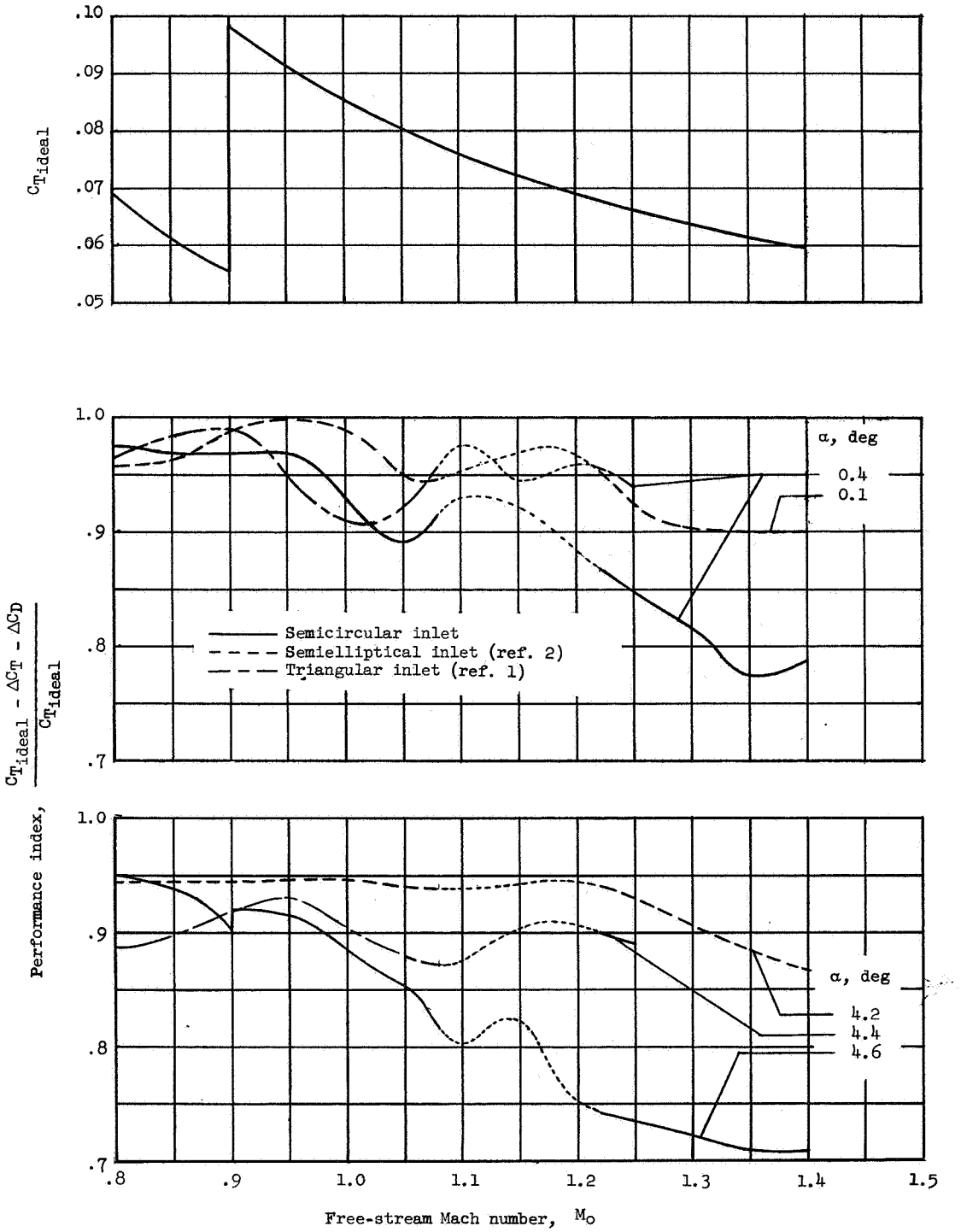

Figure 11.- Comparison of inlet performance-index variation with Mach number for semicircular inlet and inlets of references 1 and 2. Ideal thrust schedule is for turbojet engine with afterburner operating at $M_o = 0.90$ and above.

NACA-Langley